Low-Frequency Noise of nc-Si:H/c-Si Heterojunction Diodes

M. Dai, J. I. Oh, and W. Z. Shen

***Abstract*—Low-frequency noise (LFN) measurements were performed on hydrogenated nanocrystalline silicon (nc-Si:H)/crystalline-silicon heterojunction diodes for the forward- and reverse-biased currents I. The $1/f^{\gamma}$ noise with $\gamma \sim 1.3$ (for low I) or 0.6 (for high I) was observed to dominate the LFN, and the noise power spectral density S_i showed a power-law behavior ($S_i \sim I^{\alpha}$, where $\alpha \sim 2$). This quadratic behavior may indicate the $1/f^{\gamma}$ noise to stem from the carrier number fluctuations mediated by deep trap states (for $\gamma \sim 1.3$) or band tail states (for $\gamma \sim 0.6$) of nc-Si:H. Also, the band tail width of nc-Si:H was estimated to be ∼65 meV.**

***Index Terms*—Band tail states, carrier number fluctuations, deep trap states, hydrogenated nanocrystalline silicon (nc-Si:H), $1/f$ noise.**

I. Introduction

HYDROGENATED nanocrystalline silicon (nc-Si:H), Si nanocrystals dispersed in a hydrogenated amorphous Si (a-Si:H) matrix, has great potential in optoelectronic devices due to its novel properties such as quantum confinement [1], resonant tunneling [2], and visible photoluminescence [3]. These novel properties of nc-Si:H basically come from the Si nanocrystals that can be considered as quantum dots. On the other hand, the dispersion of the Si nanocrystals in a-Si:H naturally results in grain boundary defects that may lead to electronic noise. Although this undesirable electronic noise may be unavoidable, it would be of fundamental importance to understand its underlying mechanism, in turn helping design high-performance nc-Si:H-based devices.

In this letter, we investigate low-frequency noise (LFN) of nc-Si:H/crystalline silicon (c-Si) heterojunction diodes that are one of the simplest devices made of nc-Si:H, observed by the current noise measurement for both forward and reverse biases at room temperature. We show that their LFN is dominated by $1/f$ noise. We also discuss the underlying mechanism of the $1/f$ noise in terms of carrier number fluctuations mediated by bulk defect states of nc-Si:H.

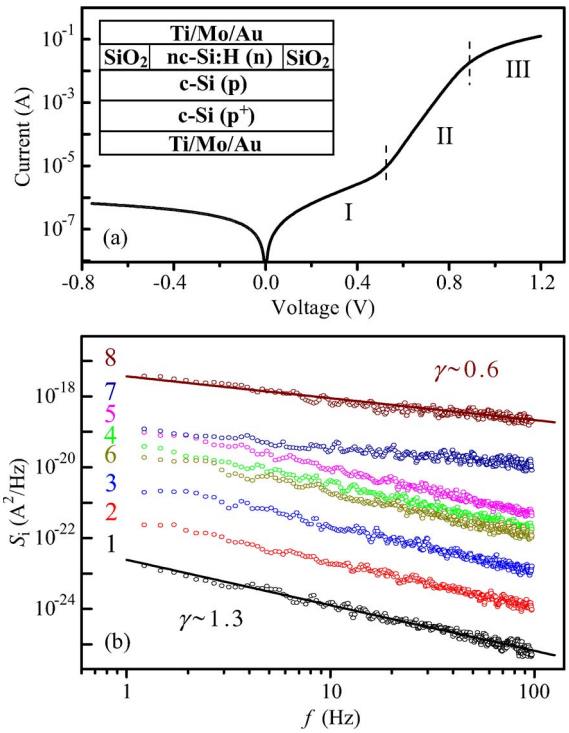

Fig. 1. (a) Semilogarithmic I–V plot. (Inset) Schematic cross-sectional view of the diodes. (b) Noise power spectral density S_i versus frequency f for various forward-biased currents I (in amperes): (1) 8.4×10^{-9}, (2) 3.2×10^{-8}, (3) 1.0×10^{-7}, (4) 4.0×10^{-7}, (5) 1.6×10^{-6}, (6) 6.4×10^{-6}, (7) 1.0×10^{-4}, and (8) 4.0×10^{-4}. Two values of the exponent γ are indicated.

II. Device Fabrication and Experimental Procedure

A cross-sectional view of nc-Si:H (n)/c-Si (p) heterojunction diodes is shown in the inset of Fig. 1(a). First, the boron-doped c-Si (111) layer of ∼7 μm thick was grown on a p^+-type c-Si (111) substrate of 300 μm thick and $\sim 2.5 \times 10^{-2}$ $\Omega \cdot$ cm by vapor phase epitaxy at 1200 °C. Second, the SiO_2 layer of ∼1 μm thick was thermally deposited on the c-Si epilayer at 1020 °C. Then, the n-type nc-Si:H layer was selectively grown within the prepatterned square (300 μm × 300 μm) by plasma-enhanced chemical vapor deposition (PECVD) at a radio frequency (13.56 MHz) power density of 0.6 W/cm^2, a dc

Manuscript received November 4, 2011; accepted November 12, 2011. Date of publication December 23, 2011; date of current version January 27, 2012. This work was supported in part by the National Major Basic Research Project under Grant 2012CB934302, and in part by the Natural Science Foundation of China under Contracts 11074169 and 11174202. The review of this letter was arranged by Editor M. Passlack.

M. Dai and W. Z. Shen are with the Laboratory of Condensed Matter Spectroscopy and Opto-Electronic Physics and the Key Laboratory of Artificial Structures and Quantum Control (Ministry of Education), Department of Physics and Institute of Solar Energy, Shanghai Jiao Tong University, Shanghai 200240, China (e-mail: daimao1986@sjtu.edu.cn; wzshen@sjtu.edu.cn).

J. I. Oh is with the Laboratory of Condensed Matter Spectroscopy and Optoelectronic Physics and the Key Laboratory of Artificial Structures and Quantum Control (Ministry of Education), Department of Physics and Institute of Solar Energy, Shanghai Jiao Tong University, Shanghai 200240, China, and also with the Department of Physics, Boston College, Boston, MA 02467 USA (e-mail: ohje@bc.edu).

Color versions of one or more of the figures in this letter are available online at http://ieeexplore.ieee.org.

Digital Object Identifier 10.1109/LED.2011.2176552

bias of -200 V to the substrate, a mixed $(SiH_4 + H_2)$ gas flow rate of 150 sccm, a chamber pressure of 150 Pa, and 250 °C. The square pattern was made by using a photolithography technique. The silane (SiH_4) content was kept at $\sim$1% of the mixed gas, and a certain level of phosphine (PH_3; $\sim$0.8% of SiH_4) was introduced for the phosphorus doping. The doping levels of c-Si (p) epilayer and nc-Si:H (n) layer were both estimated to be $\sim 10^{16}$ cm^{-3} from the four-probe resistivity measurement. The average size of nanocrystallites and the crystalline volume fraction were obtained to be $\sim$5 nm and $\sim$55% through X-ray diffraction and micro-Raman spectroscopy measurements, respectively. Lastly, Ti/Mo/Au (50/20/500 nm) electrodes were made by electron-beam evaporation.

I–V curves were obtained with a K2400 source meter. LFN measurements were performed with an SR760 fast-Fourier-transform spectrum analyzer preceded by an SR570 low-noise current preamplifier at room temperature. The current noise power spectral density S_i in square amperes per hertz was obtained as $S_i = (P - P_0)\sigma^2$, where P (P_0) is the measured current noise power spectral density in square volts per hertz with SR760 for the constant (zero-biased) current and σ is the sensitivity of SR570 in amperes per volt. To minimize external noise, the samples were kept in a home-built Faraday cage, and CdNi batteries were used as the power source.

III. Results and Discussion

An I–V curve of our diodes is presented in Fig. 1(a), showing a high rectification ratio ($> 10^3$ at $\pm$0.8 V). For the forward bias, it can be divided up into three regimes: I, II, and III. It can be found from our previous work [4] that each regime results from the recombination-dominant (I), diffusion-dominant (II), or series-resistance-affected (III) transport mechanism. Here, we will not discuss the transport mechanism of the diodes but want to focus on their LFN that is nonetheless associated with it.

The frequency-dependent current noise power spectral density S_i, measured for low frequency $(f = 1{-}100$ Hz) and forward-biased current $(I = 8.4 \times 10^{-9}{-}4.0 \times 10^{-4}$ A), is plotted in Fig. 1(b), clearly showing that $S_i \sim 1/f^{\gamma}$, i.e., $1/f^{\gamma}$ noise (or $1/f$ noise hereinafter). From the figure, one can readily see two obvious features of the noise power density. One is that the characteristic exponent γ, determined from the least squares fit, has double values ($\sim$1.3 and 0.6), depending on the current level. The other feature is that the noise power density S_i does not simply exhibit a monotonic increase upon increasing the current, e.g., curve 6 is located below curve 5. These noise features may shed light on the origin of the LFN, as will be discussed hereinafter. Note that we have also measured the f-dependent noise power density for the reverse-biased current $(I = 5.0 \times 10^{-9}{-}3.2 \times 10^{-7}$ A) which showed the $1/f$ noise with $\gamma \sim 1.3$ and also that the forward-biased current for the measurements was restricted to regimes I and II above which (i.e., the regime III) the diodes act like resistors.

From the f-dependent S_i described previously, one can construct the current-dependent S_i at a fixed frequency. For the reverse bias as in Fig. 2(b), the noise power density simply shows a monotonic power-law behavior as $S_i \sim I^{\alpha}$ with the exponent

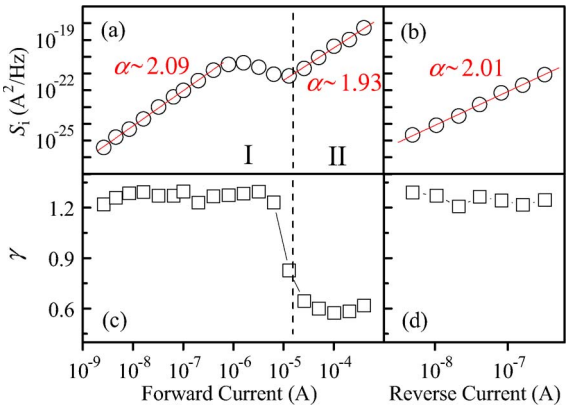

Fig. 2. Current-dependent noise power spectral density S_i for (a) forward and (b) reverse biases at $f = 20$ Hz. The solid lines are fitting functions in a form of $S_i \sim I^{\alpha}$. Current-dependent exponent γ for (c) forward and (d) reverse biases.

$\alpha = 2.01$. For the forward bias as in Fig. 2(a), on the other hand, it shows an N-shape current dependence, interestingly having a negative slope in the range of $8.0 \times 10^{-7}{-}1.3 \times 10^{-5}$ A, yet having the same power law as for the reverse bias with the exponent $\alpha = 2.09$ and 1.93 for low ($< 8.0 \times 10^{-7}$ A) and high ($> 1.3 \times 10^{-5}$ A) currents, respectively. There are primarily two fluctuation models to describe $1/f$ noise in semiconductor devices [5], i.e., mobility fluctuation model ($\Delta\mu$ model) and carrier number fluctuation model (Δn model). These two models seemingly well describe a linear ($\Delta\mu$ model) [6] or quadratic (Δn-model) [7], [8] current-dependent S_i in p-n junction diodes. Thus, the nearly quadratic power law in Fig. 2(a) and (b) may indicate that the observed $1/f$ noise is mainly attributed to carrier number fluctuations. Also, considering a relatively high density of bulk defects in nc-Si:H due to grain boundaries and structural disorders [9], the $1/f$ noise may occur through bulk-defect-assisted generation–recombination (G-R) events in the depletion region [7] (i.e., the bulk contribution) rather than surface-state-assisted G-R events in the peripheral region [10] (i.e., the surface contribution). Moreover, there are usually two mechanisms inducing carrier number fluctuations [5], i.e., carrier tunneling [11] and thermal activation [12]. The former mechanism does not appear to be applied here since it assumes surface effect as the main contribution to $1/f$ noise, leaving the latter mechanism to be appropriate in this work.

Addressing the two values of the exponent γ, we present the current-dependent γ in Fig. 2(c) and (d). It clearly shows a steplike behavior for the forward bias, i.e., $\gamma \sim 1.3$ in regime I and $\sim$0.6 in regime II, whereas it keeps $\sim$1.3 for the reverse bias. This may imply two different sources for the $1/f$ noise, depending on the current level. There are two dominant defect states in nc-Si:H [13], i.e., deep trap states near the midgap and exponential-like band tail states near the band edges. A schematic distribution of the density of states (DOS) of nc-Si:H is shown in Fig. 3(a), including two Gaussian distributions for deep trap states as in [13] and two exponential distributions for band tail states (i.e., conduction and valence band tails). Note that the assumed Gaussian distributions indicate that the deep trap states stem from Si dangling bonds [13]. Within the framework of the thermal activation mechanism [12], the

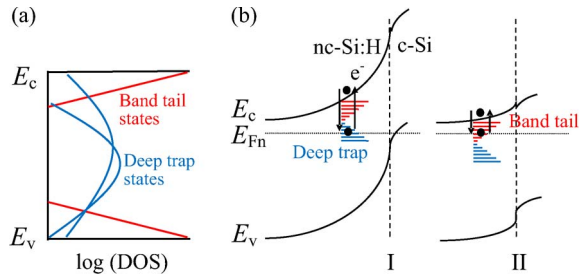

Fig. 3. (a) Schematic of the DOS of defects in nc-Si:H. E_c (E_v) is the conduction (valence) band energy. (b) Energy band diagrams in the cases of regimes (left) I and (right) II. E_{Fn} is the electron quasi-Fermi level. (Blue) Deep trap and (red) band tail states near E_{Fn} are depicted. Generation and recombination of electrons are indicated with arrows.

exponent γ can be related to the energy distribution of defect states $N(E)$ as [14]

$$N(E) = N_0 \exp\left[-(E_c - E)/E_0\right] \tag{1}$$

$$\gamma = 1 - kT/E_0 \tag{2}$$

where N_0 and E_0 are the characteristic distribution parameters and kT is the thermal energy. As can be seen from these equations and Fig. 3(a), $N(E)$ increases like the DOS of conduction band tail with E approaching E_c if $E_0 > 0$ (i.e., $\gamma < 1$), whereas it shows an opposite behavior like the DOS of deep trap if $E_0 < 0$ (i.e., $\gamma > 1$). Thus, the $1/f$ noise appears to be caused by thermally induced carrier number fluctuations mediated by the band tail states or the deep trap states of nc-Si:H for high (II) or low (I and the reverse-biased) current, respectively. Also, from (2), the characteristic parameter E_0 can be estimated to be $\sim$65 meV for the conduction band tail ($\gamma \sim 0.6$), which is in good agreement with the previous result ($\sim$62 meV) obtained through the transient photocapacitance method [15].

The change of the noise sources can be described with energy band diagrams as in Fig. 3(b). It has been known that defect states near the electron quasi-Fermi level E_{Fn} mainly contribute to mediating carrier number fluctuations [16], [17]. For a high forward bias (II), E_{Fn} may reside around the band tail states as in the right side of the figure. For a decreased forward bias (I), leading to increased band bending, E_{Fn} may now sit around the deep trap states as in the left side of the figure. For a reverse bias, the band bending becomes even larger than for regime I, keeping E_{Fn} around the deep trap states.

Finally, returning to Fig. 2(a), we want to make a remark on the negative slope of S_i. Although its underlying physics is not clearly uncovered in this work, it seems to result from the competition between the two bulk defect states since it occurs near the boundary of regimes I and II. Note also that a similar S_i behavior has been observed in 4H-SiC p-n diodes [18].

IV. Conclusion

We have fabricated nc-Si:H (n)/c-Si (p) heterojunction diodes to investigate LFN. From the current noise measurement, we have observed that the LFN is dominated by the $1/f^{\gamma}$ noise with the exponent $\gamma = 1.3$ and 0.6 and also that the noise power spectral density shows a quadratic dependence of the current. We have concluded from the latter observation that carrier number fluctuations mainly lead to LFN, whereas we have concluded from the former observation that they are mediated by two bulk defect states of nc-Si:H. Also, the current-dependent steplike exponent deviating from $\gamma = 1.0$ has allowed us to infer that deep trap and band tail states of nc-Si:H contribute to the $1/f^{\gamma}$ noise for the low and high current levels, respectively. Moreover, we have been able to extract the band tail width of nc-Si:H (i.e., $E_0 \sim 65$ meV) from the observed exponent, implying that the current noise measurement can be a useful means of characterizing materials of band tail states.

References

[1] Y. T. Tan, T. Kamiya, Z. A. K. Durrani, and H. Ahmed, "Room temperature nanocrystalline silicon single-electron transistors," *J. Appl. Phys.*, vol. 94, no. 1, pp. 633–637, Jul. 2003.

[2] W. S. Wei, T. M. Wang, and W. Z. Shen, "Tunnelling in heterojunction of n-type hydrogenated nanocrystalline silicon film with p^+-type crystal silicon," *Semicond. Sci. Technol.*, vol. 21, no. 4, pp. 532–539, Apr. 2006.

[3] Z. Yuan, A. Anopchenko, N. Daldosso, R. Guider, D. Navarro-Urrios, A. Pitanti, R. Spano, and L. Pavesi, "Silicon nanocrystals as an enabling material for silicon photonics," *Proc. IEEE*, vol. 97, no. 7, pp. 1250–1268, Jul. 2009.

[4] J. J. Lu, J. Chen, Y. L. He, and W. Z. Shen, "Band offsets and transport mechanisms of hydrogenated nanocrystalline silicon/crystalline silicon heterojunction diode: Key properties for device applications," *J. Appl. Phys.*, vol. 102, no. 6, p. 063 701, Sep. 2007.

[5] F. N. Hooge, "$1/f$ noise sources," *IEEE Trans. Electron Devices*, vol. 41, no. 11, pp. 1926–1935, Nov. 1994.

[6] T. G. M. Kleinpenning, "$1/f$ noise in p-n junction diodes," *J. Vac. Sci. Technol. A, Vac. Surf. Films*, vol. 3, no. 1, pp. 176–182, Jan./Feb. 1985.

[7] F. C. Hou, G. Bosman, E. Simoen, J. Vanhellemont, and C. Claeys, "Bulk defect induced low-frequency noise in n^+-p silicon diodes," *IEEE Trans. Electron Devices*, vol. 45, no. 12, pp. 2528–2536, Dec. 1998.

[8] A. van der Ziel, X. Zhang, and A. H. Pawlikiewicz, "Location of $1/f$ noise sources in BJTs and HBJTs—I. Theory," *IEEE Trans. Electron Devices*, vol. ED-33, no. 9, pp. 1371–1376, Sep. 1986.

[9] X. N. Liu, G. Y. Xu, Y. X. Sui, Y. L. He, and X. M. Bao, "Electron spin resonance in doped nanocrystalline silicon films," *Solid State Commun.*, vol. 119, no. 6, pp. 397–401, Jul. 2001.

[10] S. T. Hsu, D. J. Fitzgerald, and A. S. Grove, "Surface-state related $1/f$ noise in p-n junctions and MOS transistors," *Appl. Phys. Lett.*, vol. 12, no. 9, pp. 287–289, May 1968.

[11] A. L. McWhorter, "$1/f$ noise and germanium surface properties," in *Semiconductor Surface Physics*, R. H. Kingston, Ed. Philadelphia, PA: Univ. Pennsylvania Press, 1957, pp. 207–228.

[12] P. Dutta and P. M. Horn, "Low-frequency fluctuations in solids: $1/f$ noise," *Rev. Mod. Phys.*, vol. 53, no. 3, pp. 497–516, Jul. 1981.

[13] K. Lips, P. Kanschat, and W. Fuhs, "Defects and recombination in microcrystalline silicon," *Sol. Energy Mater. Sol. Cells*, vol. 78, no. 1–4, pp. 513–541, Jul. 2003.

[14] J. I. Lee, J. Brini, A. Chovet, and C. A. Dimitriadis, "On $1/f^{\gamma}$ noise in semiconductor devices," *Solid State Electron.*, vol. 43, no. 12, pp. 2181–2183, Jul. 1999.

[15] A. F. Halverson, J. J. Gutierrez, J. D. Cohen, B. Yan, J. Yang, and S. Guha, "Electronic characterization and effects of light-induced degradation on hydrogenated nanocrystalline silicon," *Appl. Phys. Lett.*, vol. 88, no. 7, p. 071 920, Feb. 2006.

[16] A. van der Ziel and E. R. Chenette, "Noise in solid state devices," *Adv. Electron. Electron Phys.*, vol. 46, pp. 313–404, 1978.

[17] R. Burgess, "The statistics of charge carrier fluctuations in semiconductors," *Proc. Phys. Soc. London, Sect. B*, vol. 69, pp. 1020–1027, Mar. 1956.

[18] S. L. Rumyantsev, A. P. Dmitriev, M. E. Levinshtein, D. Veksler, M. S. Shur, J. W. Palmour, M. K. Das, and B. A. Hull, "Generation–recombination noise in forward biased 4H-SiC p-n diodes," *J. Appl. Phys.*, vol. 100, no. 6, p. 064 505, Sep. 2006.